CMS Physics Analysis Summary

Contact: cms-pag-conveners-exotica@cern.ch 2011/03/21

Search for New Physics in Highly Boosted Z^0 Decays to Dimuons in pp Collisions at $\sqrt{s} = 7$ TeV

The CMS Collaboration

Abstract

An inclusive search for anomalous production of highly boosted Z^0 bosons in the dimuon decay channel arising from the decays of new heavy particles has been performed by the CMS Collaboration. The data correspond to an integrated luminosity of 36 pb^{-1} collected with the CMS detector from pp collisions provided by the CERN LHC at $\sqrt{s} = 7$ TeV. The search is optimized for the detection of excited quark production and decay via $q^* \to qZ^0 \to q\mu^+\mu^-$, with no explicit reconstruction of the jet recoiling against a high transverse momentum Z^0. The results are consistent with background-only expectations. Limits are derived on excited quark production in the plane of compositeness scale versus mass for two scenarios of production and decay: one assuming excited quark transitions via Standard Model gauge bosons only, and one including also novel contact interaction transitions from new strong dynamics. The mass limits at 95% confidence level with contact interactions are more sensitive than previous searches in scenarios where the coupling to gluons is suppressed relative to the electroweak gauge bosons, ruling out masses below 1.17 TeV in the extreme case when this coupling is zero.

1 Introduction

This note addresses a search for new physics that can yield an excess of events in the tail of the transverse momentum (p_{T}) spectrum of Z^0 production, measured in the dimuon decay channel. The search is potentially sensitive to a broad range of models of new physics, including quark compositeness, Supersymmetry, Technicolor, and new gauge bosons. We perform an inclusive search for highly boosted Z^0 bosons that is optimized and interpreted within one such model, the production and weak decay of excited quarks (q^*) to a quark and Z^0. A multitude of excited fermion states are an expected consequence of models of compositeness, which attempt to explain the observed mass hierarchy of quarks and fermions. Traditionally excited quarks are sought directly in hadron collisions through the dijet final state of a quark and gluon [1]. However, other decay modes are possible and should be considered in order to maintain model independence and to maximize the potential for discovery, as advocated by the LHC New Physics Working Group [2]. While the expected branching fraction to the dimuon final state is expected to be small, the search remains sensitive as it is nearly background free.

The analysis strategy centers on performing a simple counting experiment of highly boosted Z^0 bosons reconstructed in opposite sign dimuon events above an optimized p_{T} threshold. No explicit use of the shape of the p_{T} distribution from the new physics source above the threshold is made, nor of the final state jet-Z^0 invariant mass. Both of these quantities form important handles on the nature of the new physics should an excess of events be seen. We employ a data driven method for the evaluation of the Standard Model background sources by fitting a smooth functional shape to the dimuon p_{T} distribution in a control region at lower p_{T}, and extrapolate it to higher p_{T}. Any significant excess in the signal region is attributed to new physics, otherwise limits at the 95% confidence level are derived on excited quark production and decay.

2 Detector Description

The central feature of the Compact Muon Solenoid (CMS) [3] apparatus is a superconducting solenoid, of 6 m internal diameter, providing a field of 3.8 T. Within the field volume are the silicon pixel and strip trackers, the crystal electromagnetic calorimeter and the brass/scintillator hadron calorimeter. Muons are measured in gas-ionization detectors embedded in the steel return yoke.

Muons are measured in the pseudorapidity window $|\eta| < 2.4$, with detection planes made of three technologies: drift tubes in the barrel region, cathode strip chambers in the endcaps, and resistive plate chambers in the barrel and endcap. The inner tracker measures charged particles within the pseudorapidity range $|\eta| < 2.4$. It provides an impact parameter resolution of $\sim$ 15 μm and a transverse momentum (p_{T}) resolution of about 1 (2,5) % for 10 (100, 500) GeV/c particles.

The first level (L1) of the CMS trigger system, composed of custom hardware processors, selects the most interesting events in less than 3.3 μs, using information from the calorimeters and muon detectors. The high-level trigger (HLT) processor farm further decreases the event rate before data storage. The muon trigger system uses information from the muon chambers and the inner tracker (at L3 in the HLT). The data used for this search were collected using a single muon trigger that had an increasing p_{T} threshold over the course of the 2010 running period, the tightest of which was 15 GeV/c.

3 Phenomenological Model

The Lagrangian describing the gauge transitions of excited fermions is given by [4]:

$$\mathcal{L}_{\text{trans}} = \frac{1}{2\Lambda}\bar{f}^*_R\sigma^{\mu\nu}\left(g_s f_s\frac{\lambda^a}{2}G^a_{\mu\nu} + gf\frac{\tau}{2}W_{\mu\nu} + g'f'\frac{Y}{2}B_{\mu\nu}\right)f_L + h.c. \quad (1)$$

The three terms, $G^a_{\mu\nu}$, $W_{\mu\nu}$, and $B_{\mu\nu}$ describe the coupling to the SU(3), SU(2), and U(1) parts of the Standard Model, respectively. The couplings to the strong and electroweak sectors are measured in units of the strength of the Standard Model gauge couplings. It is conventional to assume that all of the new couplings are equal to the Standard Model couplings between ordinary fermions (i.e. $f = f' = f_s = 1$). The two remaining parameters in the Lagrangian are the mass of the excited quark, M_{q^*}, and the compositeness scale, Λ, which are usually taken to be equal. The excited quark model can be extended with novel four-fermion contact interaction terms due to the new strong dynamics [4]:

$$\mathcal{L}_{\text{contact}} = \frac{g^2_*}{\Lambda^2}\frac{1}{2}j^\mu j_\mu \quad (2)$$

The squared coupling constant of the contact interaction, g^2_*, is usually taken to be 4π, and j^μ represents the fermion current.

For this analysis we consider a reduced parameter space of the model consisting of 3 independent quantities: the mass of the excited quark, M_{q^*}, the compositeness scale, Λ, and the strong coupling constant f_s (we assume $f = f' = 1$). We consider only first generation excited quarks (u^*, d^*) that are degenerate in mass. We treat separately the case when excited quark transitions are mediated only by gauge boson interactions (Eq. 1), as typically assumed for excited quark searches in the dijet channel (e.g. [1]) or in excited fermion searches at HERA [5], and when contact interaction diagrams (Eq. 2) are assumed to contribute to the production and decay as in excited lepton searches at hadron colliders. The branching fraction to Z^0 for u^* (d^*) when $\Lambda = M_{\text{q}^*}$ is 3% (5%) for gauge-only couplings with $f_s = 1$, increasing to slightly over 20% (30%) with $f_s = 0$. With the inclusion of the 4-fermion contact interaction diagrams, the branching fraction is reduced to about 2% and is nearly independent of f_s. The partial width of $\text{q}^* \to qff'$ via the contact interaction has an additional $(\Lambda/M_{\text{q}^*})^2$ dependence over the gauge decays, and is thus highly suppressed for $\Lambda/M_{\text{q}^*} \gg 1$. On the other hand, $\Lambda/M_{\text{q}^*} \ll 1$ implies a very large total width since the contact interaction approximation to the new strong dynamics is no longer appropriate, and is not considered here.

4 Event Samples

The data used were recorded in 2010 when the LHC delivered pp collisions at a center-of-mass energy of 7 TeV. The results presented in this note correspond to an integrated luminosity of about 36 pb^{-1}.

The samples of electroweak processes with Z^0 and W production are produced with POWHEG [6–8] interfaced with the PYTHIA [9] parton-shower generator. QCD events with a muon in the final state are studied using PYTHIA. Events from $t\bar{t}$ + Jets and W + Jets are studied using MADGRAPH [10]. Generated events are processed through the full GEANT4 [11] detector simulation, trigger emulation and event reconstruction chain of the CMS experiment.

5 Muon Selection

The events used in this analysis were collected using a single muon trigger which requires $p_T > 9$, 11 or 15 GeV/c, depending on running period.

The reconstruction and calibration of muons follows standard CMS methods [12]. Muons can be reconstructed in the muon system as "muon stand-alone" tracks, and they can be reconstructed as tracks in the silicon tracker. The two can be matched and fit together to form a "global muon". Both muons in the event must be identified as global muons with at least 10 hits in the silicon tracker. Both muons must have $p_T > 20$ GeV/c and have a transverse impact parameter with respect to the collision point of less than 0.2 cm. We classify all muon candidates that satisfy these criteria and are reconstructed in $|\eta| < 2.4$ as "loose" muons. At least one of the two muons in each event must be "tight", with the following additional requirements. The muon must be reconstructed in $|\eta| < 2.1$. The global track fit χ^2 per degree of freedom must be less than 10. There must be at least one hit in the pixel detector and hits from muon tracking system in at least two detection planes on the track. The muon must match a L3 trigger object firing the HLT single muon path. The matching is satisfied if the L3 object is inside a cone of $\Delta R = \sqrt{(\Delta\eta)^2 + (\Delta\phi)^2} < 0.2$ around the offline reconstructed muon and the relative transverse momentum difference to be $\Delta p_T / p_T^{reco} < 1$.

Non-prompt muons from hadron decays and misidentified muons from coincidental hit patterns that can occur in a busy environment are suppressed by imposing an isolation requirement. We require that the sum of the p_T of all tracks (excluding the muon) within a narrow cone of radius $\Delta R = 0.3$, centered on the muon, be less than 10% of the p_T of the muon. On the other hand, we are interested in signal signatures with a highly boosted Z^0. The two muons from the decay will approach collinearity with increasing boost, and therefore affect the isolation criterion. Thus, we subtract the p_T of the other muon in the isolation calculation if the two muons are in a cone of radius $\Delta R = 0.3$ and the original isolation is greater than 90% of the p_T of the other muon.

The momentum scale of the muons is set using the $Z^0 \to \mu^+\mu^-$ peak and the known Z^0 boson mass. Studies of high-energy cosmic-ray events and alignment discrepancies between silicon tracker extrapolations and muon chamber positions show that for muons with $p_T > 40$ GeV scale shifts above 1% can be excluded.

More details about muon identification in CMS at $\sqrt{s}$ = 7 TeV can be found in Ref. [12].

6 Event Selection

In every event we require a reconstructed vertex with at least four associated tracks, located less than 2 cm from the center of the detector in the direction transverse to the beam and less than 24 cm in the direction along the beam. We then select events with two isolated loose muons of opposite charge and $p_T > 20$ GeV. At least one of the two muons is required to be identified as a tight muon. Both muons are required to be consistent with the reconstructed pp interaction vertex along the beam direction. Only candidates whose $\mu^+\mu^-$ invariant mass is between 60 GeV/c^2 and 120 GeV/c^2 are selected.

Figure 1 shows dimuon p_T spectrum from CMS data compared with the simulation of excited quark signals for the contact interaction and gauge production scenarios.

The event trigger efficiency is computed as the probability that at least one of the two muons satisfies both the L1 and HLT requirements. This efficiency is found to be consistent with

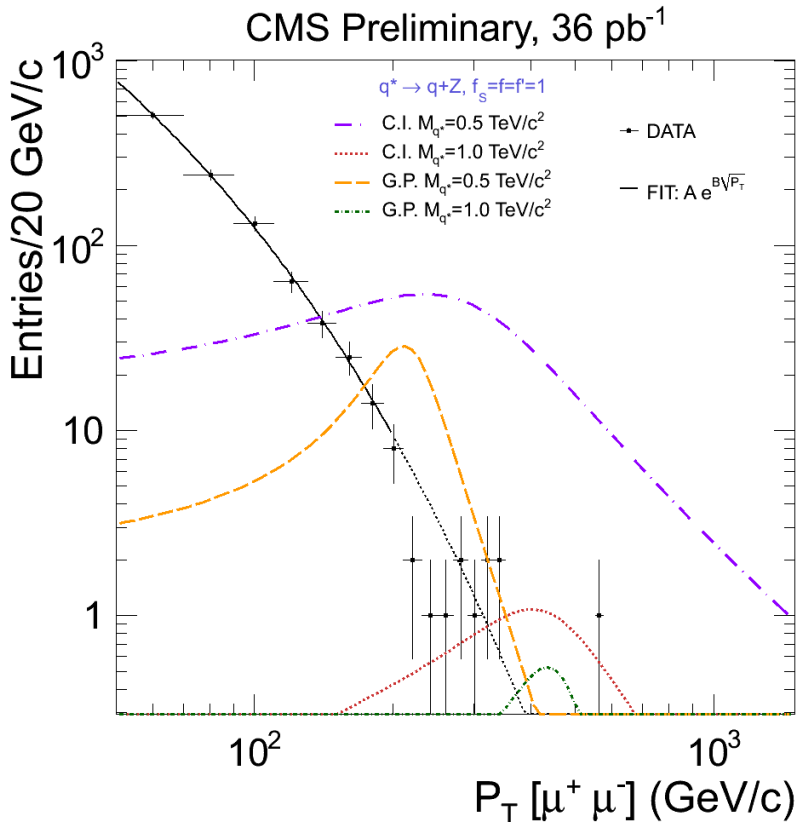

Figure 1: The dimuon p_{T} spectrum distribution from data above 50 GeV/c (dots) compared to the simulation of excited quark signals (dashed curves) normalized to the luminosity.

92% for events in which muon candidates pass the offline selection criteria and it is in good agreement with the Monte Carlo (MC) expectations.

The acceptance is defined as the probability of generator level dimuon candidates to pass the η selection ($< 2.4(2.1)$) and $p_{\mathrm{T}}^{\mu} > 20$ GeV/c and 60 GeV/c^2 $< M_{\mu^+\mu^-} <$ 120 GeV/c^2. We calculate the combined acceptance $\times$ efficiency using the sample of simulated events, as number of all of $\mu^+\mu^-$ pairs in the 60 GeV/c^2— 120 GeV/c^2 invariant mass range with both muons satisfying the selection criteria normalized to the total number of simulated events. For the excited quark production and decay scenario with contact interactions, the combined acceptance $\times$ efficiency for a $\mu^+\mu^-$ pair with $p_{\mathrm{T}} > 300$ GeV/c varies from 59% to 73% depending on the q* mass. For the scenario with only gauge production and decay, the efficiency times acceptance is higher because of the narrower decay width and varies between 69% and 74% depending on the q* mass for a $\mu^+\mu^-$ pair with $p_{\mathrm{T}} > 200$ GeV/c.

7 Backgrounds

7.1 $Z/\gamma*$ Background

The comparison between the Drell-Yan POWHEG at Next to the Leading Order (NLO) Monte Carlo (MC) and the data shows that the simulation systematically underestimates the data for $p_{\mathrm{T}} > 100$ GeV/c. The "Fully Exclusive W,Z Production" (FEWZ [13]) program predicts the cross section, which is higher than the POWHEG predictions in the region of $p_{\mathrm{T}} > 100$ GeV/c and therefore suggests a better agreement with the data. Since POWHEG MC does not provide an accurate prediction of the Drell-Yan background events and FEWZz can only calculate a pure NLO (NNLO) cross section, which does not account for detector efficiency and resolution, for the purposes of this paper we opt for a data-driven technique by directly fitting the data. We predict the shape of the $\mu^+\mu^-$ transverse momentum spectrum in the signal region from Drell-Yan production using a Monte Carlo (MC) simulation based on POWHEG event generator. From MC we derive an equation to apply on data:

$$F(p_{\mathrm{T}}) = A \cdot e^{-B\cdot\sqrt{p_{\mathrm{T}}}}. \tag{3}$$

The derived parameterization model is used to fit the data in the range $p_{\mathrm{T}} \in [50-200]$ GeV/c. We evaluate the number of background events above any optimized p_{T} thresholds relying on the fit extrapolation. As the reader can observe from Figure 1, Equation 3 seems to adequately describe the Drell-Yan p_{T} spectrum ($\chi^2/ndf = 30.24/40$, probability=89.17%). The extrapolation into signal region becomes important when a signal may be observed. Thus, several sources of uncertainties arising from the extrapolation procedure are investigated. We assign a systematic error to the events estimation by varying the fit parameters inside the errors returned by the fitting procedure. An additional systematics error is obtained by using different p_{T} ranges, $p_{\mathrm{T}} \in [50-150]$ GeV/c and $p_{\mathrm{T}} \in [50-175]$ GeV/c, to perform the fit and comparing the background events estimation to the ones from the default choice, $p_{\mathrm{T}} \in [50-200]$ GeV/c. In addition to the default fitting function in Equation (3), we checked few more shapes which were used for the dijet resonance search [1] and also give good fit of the dimuon p_{T} spectrum. The last systematic error is then computed by comparing the background events estimation obtained from all the different parametrization models.

The three contributions are summed in quadrature and used to assign the error to the estimated number of Drell-Yan background events. The final background events estimation compared to the data counting is reported in Table 1.

Table 1: Expected background for several values of the p_T cut (GeV/c) and relative systematic error assignment due to fit parameters variation inside their errors, by varying the p_T range for the fit and by using different parametrization for the fitting curves.

p_T cut (GeV/c)	> 200	> 250	> 300	> 350	> 400	> 450	> 500
Fit Parameters	$\pm$2.5	$\pm$1.2	$\pm$0.6	$\pm$0.3	$\pm$0.15	$\pm$0.07	$\pm$0.03
Different p_T Ranges	$\pm$2.1	$\pm$1.0	$\pm$0.5	$\pm$0.2	$\pm$0.11	$\pm$0.05	$\pm$0.02
Different Fit Curves	$\pm$9.6	$\pm$5.1	$\pm$2.5	$\pm$1.2	$\pm$0.55	$\pm$0.25	$\pm$0.11
Final Estimation	19.5$\pm$10.1	7.3$\pm$5.3	3.0$\pm$2.6	1.3$\pm$1.3	0.57$\pm$0.58	0.26$\pm$0.27	0.11$\pm$0.12
Data Counting	16	9	5	1	1	1	1

We investigated if the chosen template function could fit away the signal. By generating pseudo-experiments we artificially introduced an increasing fraction of signal events in order to check how the fit in the range of $p_T \in [50 - 200]$ GeV/c would be affected. It was found that for the model with the highest expected signal contribution, contact interaction with $M_{q^*} = 0.5$ TeV/c^2, the fit would absorb less than 1 % of the signal.

7.2 Other Backgrounds with Prompt Muons

Other sources of events with two prompt muons are $t\bar{t}$, tW, diboson, and $Z \to \tau\tau$ production. For a dimuon transverse momentum cut of $p_T > 70$ GeV/c, it is observed that the main contribution is coming from the $t\bar{t}$ process. The muons originate from W boson decays, which can also give rise to events with an electron and a muon. Thus the transverse momentum spectrum from $e^{\pm}\mu^{\mp}$ events should have the same shape as that of $\mu^+\mu^-$ events but without significant contamination from Drell-Yan production. For this study, the muon is selected by requesting it to pass the "tight" selection criteria. The electron is selected by using the same selection as described in Ref. [14].

The number of $e^{\pm}\mu^{\mp}$ events is expected to be twice the number of $\mu^+\mu^-$ events. By using MC we correct for unequal acceptance and efficiency due to the different selections and the mixture of two lepton flavors. The estimated ratio of $\mu^+\mu^-$ to $e^{\pm}\mu^{\mp}$ events is 0.72. For a transverse momentum above 70 GeV/c the measured number of $e^{\pm}\mu^{\mp}$ pairs is 9. Thus, the expected number of $\mu^+\mu^-$ events is 6.5. This expectation is statistically compatible with the pure MC prediction of 5.9 ± 2.4 events. For a transverse momentum cut on the dimuon candidates above 200 GeV/c, the expected $t\bar{t}$ contribution is less than 1 event.

7.3 Events with Non-Prompt Muons

In order to estimate the residual contribution from background events with at least one non-prompt or misidentified muon we select events from our data sample with single muons that pass all selection cuts except the isolation requirement. This technique was already successfully employed in Reference [15]. The idea is to create a map of the probability that these muons are isolated as a function of p_T and η. Then correct this probability map for the expected contribution from events with single prompt muons from $t\bar{t}$ and W decays and for the observed correlation between the probabilities for two muons in the same event. We use this probability map to predict the number of events with two isolated muons based on the sample of events that have two non-isolated muons. The procedure is validated using simulated events. From our data we find that on average there should be 0.270 ± 0.085 (0.0) background events from this source for a dimuon $p_T > 70$ (200) GeV/c.

8 Dimuon Transverse Momentum Spectrum

The measured $\mu^+\mu^-$ transverse momentum spectrum, for an invariant mass cut 60 GeV/c^2 < $M_{\mu\mu}$ < 120 GeV/c^2, is displayed in Figure 1 for $p_T > 50$ GeV/c. The total number of events observed for $p_T > 50$ GeV/c is 1040.

The observed and expected event yields for $p_T > 200$ GeV/c are listed in Table 2. Contributions from Drell-Yan, $t\bar{t}$ and QCD are estimated using the described data driven techniques, while W+Jets, $Z/\gamma^* \to \tau^+\tau^-$ and diboson are obtained from MC and normalized to expected cross-sections.

Table 2: Number of $\mu^+\mu^-$ events with invariant mass between 60 GeV/c^2 and 120 GeV/c^2.

source	Number of Events, $p_T > 200$ GeV/c
CMS DATA	16
$Z/\gamma^* \to \mu^+\mu^-$	19.5 ± 10.1
$t\bar{t}$ + Jets	0.25 ± 0.5
W + Jets	0 ± 0
QCD	0 ± 0
$Z/\gamma^* \to \tau^+\tau^-$	0 ± 0
diboson	0.22 ± 0.47

The highest p_T event found in data is at around 555 GeV/c. The correspondent event display is shown in Figure 3.

9 Limits

The data show no significant excess over the Standard Model expectation in the signal region of the Z^0 transverse momentum spectrum. We set limits using a simple counting of events above a certain p_T threshold and calculate the Bayesian 95% C.L. upper limit on the cross section assuming Poisson statistics for the observed yield [16] and flat prior for the cross section of the process of interest. The p_T threshold is optimized to give the best limit depending on the model, and varies between 200 to 400 GeV/c. The limit setting procedure also incorporates the systematic uncertainties on the inputs, namely those associated to the integrated luminosity, the signal acceptance $\times$ efficiency, and the expected background yield. The integrated luminosity has largest systematic uncertainty with a current precision of 11% [17].

The acceptance $\times$ efficiency to signal is calculated using full detector simulation. The corresponding systematic uncertainty is assigned to be a square sum of uncertainty on the detector acceptance and uncertainty on the efficiency of the selection criteria:

$$\delta\epsilon = \sqrt{\delta A^2 + \delta e^2}$$

Uncertainty on the acceptance was found to be on the order of 2 % in a wide range of the Z^0 p_T above 100 GeV/c. The leading source of uncertainty on the selection efficiency is attributed to the cut of 20 GeV/c on muon p_T as it causes the highest ($\sim$10%) inefficiency. This uncertainty is directly related to the performance of the muon momentum reconstruction. We compare the muon momentum scale and resolution in data and in simulation. The maximum discrepancy between the two is found to be $\sim$ 0.4% for the momentum scale and $\sim$ 25% for the Z^0 mass resolution which is assumed to be equal to the muon momentum resolution. Correcting the muon momentum scale by varying the p_T cut leads to a $\sim$ 0.1% change in the efficiency for all of the models. Correcting the muon p_T by 25% towards the true value gains $0.6 - 1.3$%

efficiency, depending on the model. We take a conservative 1.5% flat uncertainty for the efficiency of all of the models. Table 3 summarizes the uncertainties.

Table 3: Sources of systematic uncertainties

quantity	uncertainty
acceptance (A)	2%
selection (e)	1.5%
resulting efficiency (ϵ)	2.5%

We estimate the background yield in the signal region ($p_{\mathrm{T}} > 200$ GeV/c) by extrapolating a background fit into the region of interest. The corresponding systematic error on the expected background yields is explained in detail in Section 7.1.

In Figure 2 we report the final upper limit contours for the cross section times the branching fraction for the two production scenarios of q* : gauge production and contact interaction. The contours are shown in the M_{q^*} and Λ plane for the different variations of the strong coupling, f_s . Under the standard assumptions for the parameters ($M_{\mathrm{q}^*} = \Lambda$, f$= f' = f_s = 1$) we rule out the excited quarks with a mass below 911 GeV/c^2 for the gauge production q* production and 1116 GeV/c^2 for the contact interaction q* production.

For q^* created through the contact interaction scenario, we exclude a large section of the strong coupling phase space, including $f_s = 0$ with a mass up to 1170 GeV/c^2, much larger than the $f_s = 0$ limit of 252 GeV/c^2 set by H1 [5] in ep collisions. For q^* created through gauge production, these limits are the worlds best up to f_s of 0.68, with a mass of 860 GeV/c^2.

10 Conclusion

We have performed a search for highly boosted Z^0 bosons in the dimuon decay channel with the CMS detector using 36 pb^{-1}of proton-proton collision data collected at $\sqrt{s} = 7$ TeV. The Z^0 transverse momentum distribution is consistent with Standard Model expectations, and no evidence of new heavy particles decaying to Z^0 is observed so far. Limits are derived on excited quark production and decay in this weak decay mode, and we report 95% exclusion contours in the compositeness scale versus excited quark mass plane for two production scenarios and for several choices of the relative coupling to gluons.

For q^* created through the contact interaction scenario, we exclude a large section of the strong coupling phase space, including $f_s = 0$ with a mass up to 1170 GeV/c^2, much larger than the $f_s = 0$ limit of 252 GeV/c^2 set by H1 [5] in ep collisions. We can extrapolate this to the standard coupling scenario ($M_{q^*} = \Lambda$, $f = f' = f_s = 1$) where we set a limit of 1116 GeV/c^2.

For q^* created through gauge production, we also exclude portions of phase space previously not excluded. Under the standard couplings, we set the q* mass lower limit of 911 GeV/c^2, which is in agreement with the dijet resonance searches [1]. These limits are the worlds best up to f_s of 0.68, with a mass of 860 GeV/c^2.

Acknowledgments

We would like to congratulate our colleagues in the CERN accelerator departments for the excellent performance of the LHC machine. We thank the technical and administrative staff at CERN and other CMS institutes, and acknowledge support from: FMSR (Austria); FNRS and FWO (Belgium); CNPq, CAPES, FAPERJ, and FAPESP (Brazil); MES (Bulgaria); CERN;

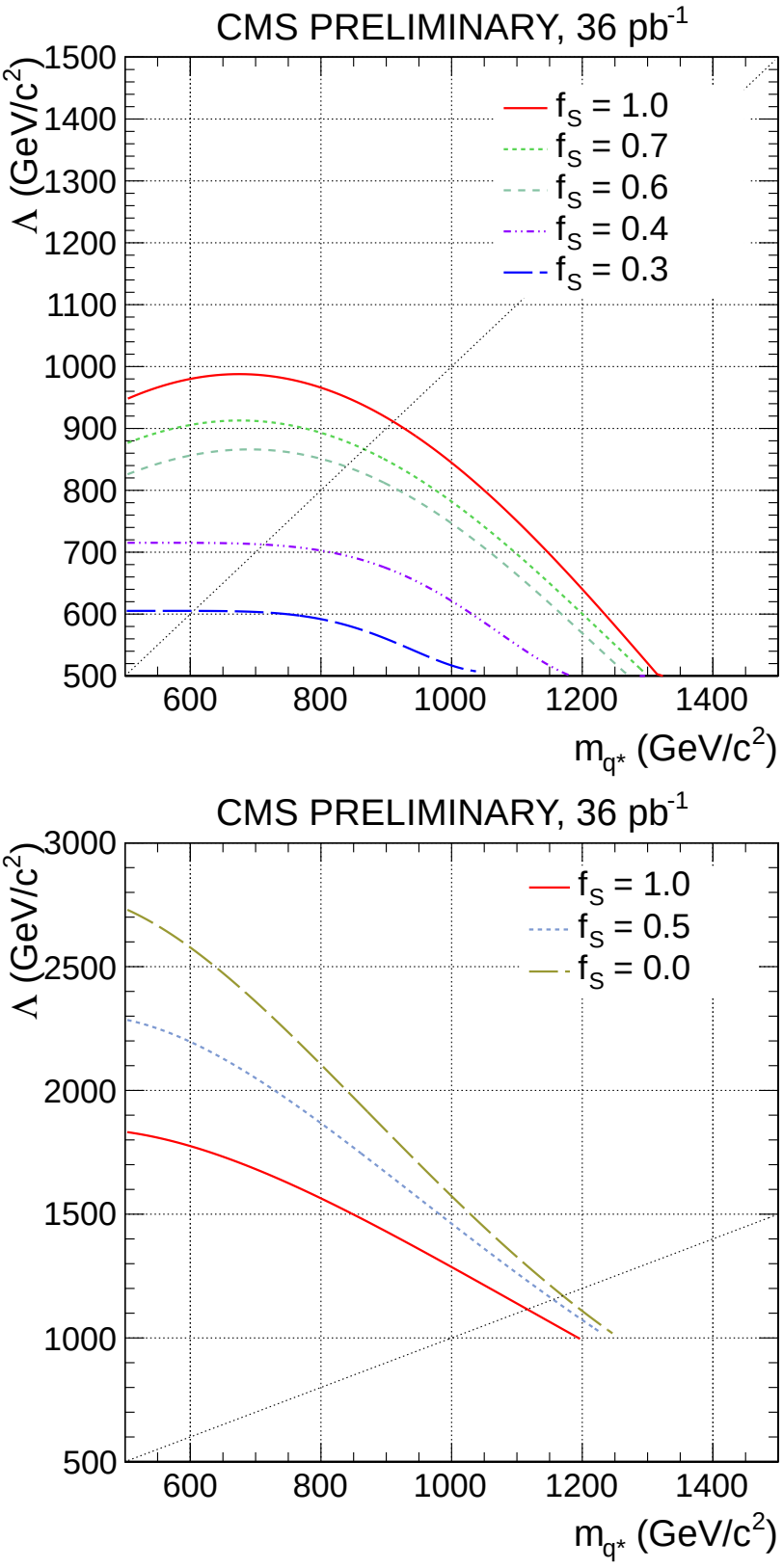

Figure 2: Contours of excluded parameters of the gauge production (top) and contact interaction (bottom) q^* production mechanisms.

CAS, MoST, and NSFC (China); COLCIENCIAS (Colombia); MSES (Croatia); RPF (Cyprus); Academy of Sciences and NICPB (Estonia); Academy of Finland, ME, and HIP (Finland); CEA and CNRS/IN2P3 (France); BMBF, DFG, and HGF (Germany); GSRT (Greece); OTKA and NKTH (Hungary); DAE and DST (India); IPM (Iran); SFI (Ireland); INFN (Italy); NRF and WCU (Korea); LAS (Lithuania); CINVESTAV, CONACYT, SEP, and UASLP-FAI (Mexico); PAEC (Pakistan); SCSR (Poland); FCT (Portugal); JINR (Armenia, Belarus, Georgia, Ukraine, Uzbekistan); MST and MAE (Russia); MSTD (Serbia); MICINN and CPAN (Spain); Swiss Funding Agencies (Switzerland); NSC (Taipei); TUBITAK and TAEK (Turkey); STFC (United Kingdom); DOE and NSF (USA).

References

[1] CMS Collaboration, "Search for Dijet Resonances in 7 TeV pp Collisions at CMS", *Phys. Rev. Lett.* **105** (2010) 211801, arXiv:1010.0203. doi:10.1103/PhysRevLett.105.211801.

[2] LHC New Physics Working Group, http://lhcnewphysics.org/web/Overview.html.

[3] CMS Collaboration, "The CMS experiment at the CERN LHC", *JINST* **3** (2008) S08004. doi:10.1088/1748-0221/3/08/S08004.

[4] U. Baur, M. Spira, and P. M. Zerwas, "EXCITED QUARK AND LEPTON PRODUCTION AT HADRON COLLIDERS", *Phys. Rev.* **D42** (1990) 815–824. doi:10.1103/PhysRevD.42.815.

[5] H1 Collaboration, "Search for Excited Quarks in ep Collisions at HERA", *Phys. Lett.* **B678** (2009) 335–343, arXiv:0904.3392. doi:10.1016/j.physletb.2009.06.044.

[6] S. Alioli, P. Nason, C. Oleari et al., "NLO vector-boson production matched with shower in POWHEG", *JHEP* **07** (2008) 060, arXiv:0805.4802. doi:10.1088/1126-6708/2008/07/060.

[7] P. Nason, "A new method for combining NLO QCD with shower Monte Carlo algorithms", *JHEP* **11** (2004) 040, arXiv:hep-ph/0409146. doi:10.1088/1126-6708/2004/11/040.

[8] S. Frixione, P. Nason, and C. Oleari, "Matching NLO QCD computations with Parton Shower simulations: the POWHEG method", *JHEP* **11** (2007) 070, arXiv:0709.2092. doi:10.1088/1126-6708/2007/11/070.

[9] T. Sjostrand, S. Mrenna, and P. Z. Skands, "PYTHIA 6.4 Physics and Manual", *JHEP* **05** (2006) 026, arXiv:hep-ph/0603175.

[10] F. Maltoni and T. Stelzer, "MadEvent: Automatic event generation with MadGraph", *JHEP* **02** (2003) 027, arXiv:hep-ex/0208156.

[11] GEANT4 Collaboration, "GEANT4: A simulation toolkit", *Nucl. Instrum. Meth.* **A506** (2003) 250–303. doi:10.1016/S0168-9002(03)01368-8.

[12] CMS Collaboration, "Performance of CMS muon identification in pp collisions at $\sqrt{s} = 7$ TeV", *CMS PAS* **MUO-2010-002** (2010).

[13] K. Melnikov, F. Petriello, Phys. Rev. D74, (2006) 114017.

[14] CMS Collaboration, "Search for Resonances in the Dielectron Mass Distribution in pp collisions at $\sqrt{s}$ = 7 TeV", *CMS PAS* **EXO-10-012** (2010).

[15] CMS Collaboration, "Search for Resonances in the Dimuon Mass Distribution in pp collisions at $\sqrt{s}$ = 7 TeV", *CMS PAS* **EXO-10-013** (2010).

[16] Particle Data Group Collaboration, "Review of particle physics", *J. Phys.* **G37** (2010) 075021. doi:10.1088/0954-3899/37/7A/075021.

[17] CMS Collaboration, "Measurement of CMS Luminosity", *CMS PAS* **EWK-10-004** (2010).

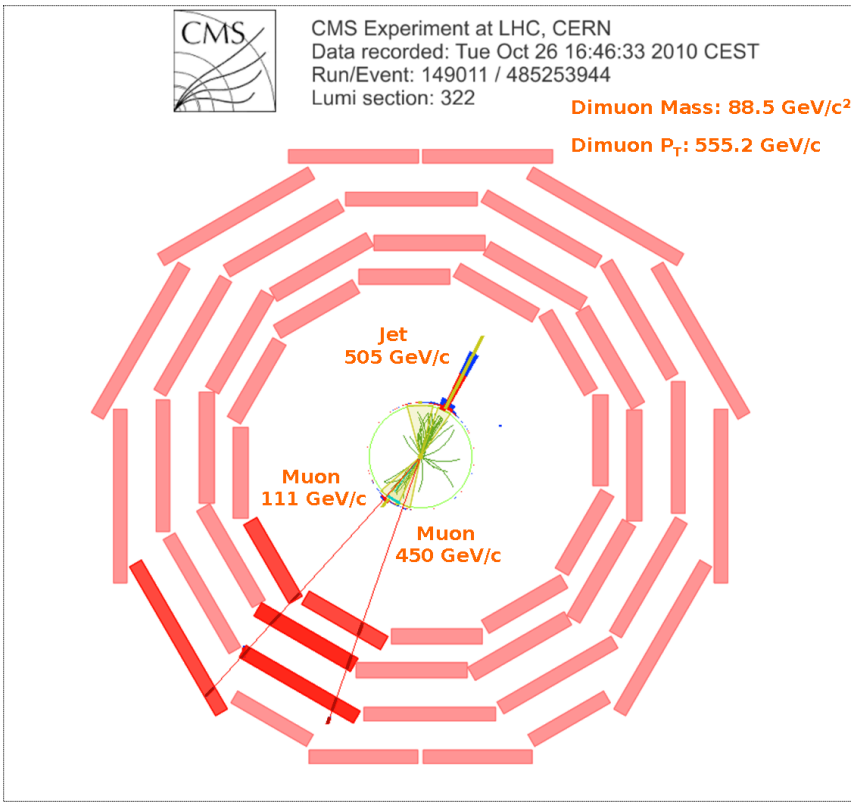

Figure 3: Event display of the highest dimuon candidate. Display in the r-ϕ plane.